*Monografías del Semin. Matem. García de Galdeano.* **27:** 307–314, (2003).

# Numerical simulation of runoff over dry beds

P. Garcia-Navarro, J. Burguete and R. Aliod

Fluid Mechanics. C.P.S. University of Zaragoza, 50015 Zaragoza, Spain.

**Abstract**

A numerical model for unsteady shallow water flow over initially dry areas is applied to a case study in a small drainage area at the Spanish Ebro river basin. Several flood mitigation measures (reforestation, construction of a small reservoir and channelization) are simulated in the model in order to compare different extreme rainfall-runoff scenarios.

**Keywords**: Shallow water flow, Conservative scheme, Upwind method

**AMS Classification**: 75F2359

## 1 Introduction

Many problems of flood routing, river management and civil protection consist of the evaluation of the maximum water levels and discharges that may be attained at particular locations during the development of an exceptional meteorological event. There is another category of events of catastrophic nature whose effects also fall into the civil protection area. In all cases it is the prevision of the scenario subsequent to the appearance and transport of a great volume of liquid onto a lower water stream. The situation can also include the case in which the stream is originally dry. There are works based on scaled physical models of natural valleys, but they represent too expensive efforts not devoid of difficulties. Therefore, there a necessity to develop adequate numerical models able to reproduce situations originated by the irregularities of a non-prismatic and sometimes dry bed. It is also necessary to trace their applicability considering the difficulty of developing a model capable of producing solutions of the complete equations despite the irregular character of the river bed.

Hydrograph or flood routing has usually been treated assuming as relevant only the main direction of the valley. For many practical applications it is accepted that the unsteady flow of water in a one-dimensional approach is governed by the shallow water (or St. Venant) equations. These represent the conservation of mass and momentum along

the direction of the main flow. Dynamic routing involves the unsteady flow assumption and the resolution of the full dynamic equations. In the field of computational hydraulics, where the modelling can be dominated by the effects not only of source terms, but also of quantities which vary spatially but independently of the flow variables, it has traditionally been difficult to have only one method able to reproduce automatically any general situation. The numerical modelling of unsteady flow in rivers is a complicated task and the difficulties grow as the pretensions to obtain better quality or more general solutions do.

The study was carried out over a rural area which was being transformed into an irrigated agriculture area to analyze the feasibility of several remediation strategies intended to reduce the damage that overflow in the creeks due to extreme rainfall events could cause on the near fields. The necessary investment for the works and launching of pressure distribution and irrigation systems required an estimation of the risk due to flood events associated to rains likely to occur in the amortization period.

The draining system analyzed in this work consists of a main creek (Valdecarro), about 12 Km long , running across the area, draining the upstream part and carrying rain waters to the downstream Arba de Luesia river. Five secondary and relatively short tributary creeks join the torrent and add their own discharge hydrographs at different lagging times.

# 2 The mathematical model

The dynamic open channel flow equations (shallow water equations) of practical application in Hydraulics can be written as the following 1D hyperbolic systems with source terms [Chow et al. (1994)], [Toro (2001)]:

$$\frac{\partial \vec{u}(x,t)}{\partial t} + \frac{d\vec{F}(x,\vec{u})}{dx} = \vec{H}(x,\vec{u}) \tag{2.1}$$

where

$$\vec{u} = \begin{pmatrix} A \\ Q \end{pmatrix}, \quad \vec{F} = \begin{pmatrix} Q \\ \frac{Q^2}{A} + gI_1 \end{pmatrix}, \quad \vec{H} = \begin{pmatrix} q_L \\ g[I_2 + A(S_0 - S_f)] \end{pmatrix}$$

and where $Q$ is the discharge, $A$ is the wetted cross section, $q_L$ is the lateral discharge, $g$ is the acceleration of gravity and $S_0$ is the bed slope. $I_1$ and $I_2$ account for hydrostatic pressure forces

$$I_1(x,A) = \int_0^{h(x,A)} [h(x,A) - z]\sigma(x,z)dz, \quad I_2(x,A) = \int_0^{h(x,A)} [h(x,A) - z]\frac{\partial \sigma(x,z)}{\partial x}dz$$

($h$ being the water depth and $\sigma$ being the channel width at a position $z$ from the bottom) $S_f$ is associated to bed friction and represented by the empirical Manning law ([Chanson (1999)]):

$$S_f = \frac{n^2 Q^2 P^{\frac{4}{3}}}{A^{\frac{10}{3}}}$$

where $n$ is the Manning coefficient of bed roughness, here assumed in SI units, and $P$ is the wetted perimeter.

From the equations in conservative form (2.1), it is possible to pass to an associated non-conservative form using

$$\frac{d\vec{F}(x,\vec{u})}{dx} = \frac{\partial \vec{F}(x,\vec{u})}{\partial x} + \frac{\partial \vec{F}(x,\vec{u})}{\partial \vec{u}}\frac{\partial \vec{u}}{\partial x} = \frac{\partial \vec{F}(x,\vec{u})}{\partial x} + \mathbf{J}(x,\vec{u})\frac{\partial \vec{u}}{\partial x}$$

where $\mathbf{J} = \frac{\partial \vec{F}}{\partial \vec{u}}$ is the Jacobian matrix of the original system. Redefining the source term as

$$\vec{H}'(x,\vec{u}) = \vec{H}(x,\vec{u}) - \frac{\partial \vec{F}(x,\vec{u})}{\partial x}$$

the non-conservative form is obtained:

$$\frac{\partial \vec{u}(x,t)}{\partial t} + \mathbf{J}(x,\vec{u})\frac{\partial \vec{u}(x,t)}{\partial x} = \vec{H}'(x,\vec{u}) \tag{2.2}$$

The characteristic form of the equations, important for the correct formulation of upwind schemes and boundary conditions, is obtained from a diagonalization of the Jacobian in (2.2). Calling $\mathbf{P}$ and $\mathbf{P}^{-1}$ the matrices that make diagonal $\mathbf{J}$,

$$\mathbf{J} = \mathbf{P}\mathbf{\Lambda}\mathbf{P}^{-1}, \;\; \mathbf{\Lambda} = \mathbf{P}^{-1}\mathbf{J}\mathbf{P}$$

Then,

$$\frac{\partial \vec{w}(x,t)}{\partial t} + \mathbf{\Lambda}(x,\vec{w})\frac{\partial \vec{w}(x,t)}{\partial x} = \mathbf{P}^{-1}(x,\vec{w})\vec{H}'(x,\vec{w}) \tag{2.3}$$

# 3 Numerical method

A conservative method is used in which a numerical flux $\vec{F}_i^T$ and a numerical source term $\vec{H}_i^T$ are defined at the grid nodes. The difference in the flux between two nodes as well as the source terms can be decomposed into parts affecting the nodes on the left and right so that the following formulation for the conservative scheme is proposed

$$\frac{\Delta \vec{u}_i^n}{\Delta t} = \vec{G}^L_{i-\frac{1}{2}} + \vec{G}^R_{i+\frac{1}{2}} \tag{3.4}$$

Defining $\vec{G}$ as

$$\vec{G}_{i+1/2} \equiv \left(\vec{H} - \frac{\delta \vec{F}}{\delta x}\right)_{i+\frac{1}{2}} \equiv \left(\vec{H}' - \mathbf{J}\frac{\delta \vec{u}}{\delta x}\right)_{i+\frac{1}{2}} \tag{3.5}$$

For the applications presented in this work, a second order in space and time upwind TVD scheme has been used. The choice is justified by a previous numerical study on the performance of a series of methods, which gave as conclusion that this scheme was the one providing the best performance for unsteady flow over irregular valleys. In this scheme the above decomposition is identified with left ($\vec{G}^-$) and right ($\vec{G}^+$) moving contributions:

$$\vec{G}^R_{i+\frac{1}{2}} = \left(\vec{G}^-\right)^n_{i+\frac{1}{2}} + \frac{\Delta t}{2}\left\{\left[\mathbf{\Psi}^+\left(1-\frac{\Delta t}{\delta x}\mathbf{J}^+\right)\vec{G}^+\right]^n_{i-\frac{1}{2}} - \left[\mathbf{\Psi}^-\left(1+\frac{\Delta t}{\delta x}\mathbf{J}^-\right)\vec{G}^-\right]^n_{i+\frac{3}{2}}\right\}$$

$$\vec{G}^L_{i+\frac{1}{2}} = \left(\vec{G}^+\right)^n_{i+\frac{1}{2}} + \frac{\Delta t}{2}\left\{\left[\mathbf{\Psi}^-\left(1+\frac{\Delta t}{\delta x}\mathbf{J}^-\right)\vec{G}^-\right]^n_{i+\frac{3}{2}} - \left[\mathbf{\Psi}^+\left(1-\frac{\Delta t}{\delta x}\mathbf{J}^+\right)\vec{G}^+\right]^n_{i-\frac{1}{2}}\right\}$$

with:

$$\mathbf{J}^\pm = \mathbf{P}\begin{pmatrix} \frac{1\pm\text{sign}(v+c)}{2} & 0 \\ 0 & \frac{1\pm\text{sign}(v-c)}{2} \end{pmatrix}\mathbf{P}^{-1}\mathbf{J}$$

$$\vec{G}^\pm = \mathbf{P}\begin{pmatrix} \frac{1\pm\text{sign}(v+c)}{2} & 0 \\ 0 & \frac{1\pm\text{sign}(v-c)}{2} \end{pmatrix}\mathbf{P}^{-1}\vec{G}$$

Making an implicit treatment of the source term, necessary to avoid the numerical instabilities produced by dominant source terms, the scheme is:

$$\begin{aligned}\left(1-\mathbf{K}^n_i\frac{\Delta t}{2}\right)\Delta\vec{u}^n_i = \Delta t\left[\left(\vec{G}^+\right)^n_{i-\frac{1}{2}} + \left(\vec{G}^-\right)^n_{i+\frac{1}{2}}\right] \\ +\frac{\Delta t}{2}\left\{\left[\mathbf{\Psi}^+\left(1-\frac{\Delta t}{\delta x}\mathbf{J}^+\right)\vec{G}^+\right]^n_{i-\frac{1}{2}} - \left[\mathbf{\Psi}^+\left(1-\frac{\Delta t}{\delta x}\mathbf{J}^+\right)\vec{G}^+\right]^n_{i-\frac{3}{2}}\right. \\ \left.+\left[\mathbf{\Psi}^-\left(1+\frac{\Delta t}{\delta x}\mathbf{J}^-\right)\vec{G}^-\right]^n_{i+\frac{1}{2}} - \left[\mathbf{\Psi}^-\left(1+\frac{\Delta t}{\delta x}\mathbf{J}^-\right)\vec{G}^-\right]^n_{i+\frac{3}{2}}\right\}\end{aligned} \tag{3.6}$$

with $\mathbf{K}$ the Jacobian of the source term and $\mathbf{\Psi}$ the limiting function matrix necessary to avoid numerical oscillations. For more details on this scheme see [Burguete (2001)].

## 3.1 Numerical boundary conditions

The method implemented to defie the numerical boundary conditions at the inlet and outlet is based on a very important physical principle: the increment of mass in the whole system in a time interval is the result of the entering mass flow minus the leaving mass flow during that period of time.

In one time step, the numerical scheme as defined in (3.6) supplies updated values for all the nodal variables and the difference respect to the net incoming flow rate is the volume error of the numerical scheme. It can be seen as if the scheme was generating a numerical inflow volume $V^{num}_{in} = Q^n_1\Delta t$ and a numerical outflow volume $Q^{num}_{out} = Q^n_N\Delta t$. In order to achieve perfect volume conservation, if the upstream physical boundary condition is $Q^{n+1}_1$ at the inlet it is assumed that the physical volume entering during one time step is $V^{phy}_{in} = \frac{1}{2}\left(Q^{n+1}_1 + Q^n_1\right)\Delta t$, then the corrected value for the wetted section upstream $A^{n+1}_1$ is

$$A^{n+1}_1 = A^s_1 + \frac{V^{phy}_{in} - V^{num}_{in}}{\delta x} = A^s_1 + \frac{1}{2}\left(Q^{n+1}_1 - Q^n_1\right)\frac{\Delta t}{\delta x}$$

and for the wetted section downstream $A^{n+1}_N$ is

$$A^{n+1}_N = A^s_N - \frac{1}{2}\left(Q^{n+1}_N - Q^n_N\right)\frac{\Delta t}{\delta x}$$

### 3.2 Front advance over dry bed

Unsteady shallow water flow over dry beds is at present one of the topics of research in computational hydraulics. One way to deal with this kind of flow is to use a moving computational mesh so that computation is only performed in the wet cells and the grid moves as the water front does. Suitable boundary conditions must be applied for the correct front tracking. A different approach consists of a through calculation of the front position as it advances over a computational mesh covering all the physical domain and in which there are both wet and dry cells. The option chosen in this work is based on the empirical correlation proposed by Strickler in 1923 for the Manning coefficient in rivers

$$n = 0.041 d_{50}^{1/6}$$

Given an estimation for the global or local Manning coefficient, the above relation supplies the order of magnitude of $d_{50}$. In our model, this value is used as the minimum water depth required at the front position to allow front advance. For water depths below that value, water is forced to stop and accumulate.

## 4 Risk remediation strategies and numerical results

For this simulation the discharge hydrograph at the upstream end of the creek was used as physical boundary condition and subsequent hydrographs, entering Valdecarro creek through its confluences, were considered as lateral discharges during a 5 hour flooding. From the beginning of this study, the lower part was identified as problematic and a preliminary decision of performing a channelization in the last 3 Kms was made. As for the roughness characterization, all the reaches were given an average value of Manning's n=0.03

In a first calculation, the basic magnitudes defining the torrent were used to evaluate the extent of the flooding in presence of the actual physical and hydrologic conditions as well as the mentioned channelization. The valley cross section shape was known up to a limit in width. From that point, vertical walls were assumed, that is, no real flood plain was simulated. The results indicated that the banks were not able to convey the water in the middle part under the assumed rain hypothesis. The discharge hydrographs were deduced from standard hydrologic hypothesis. Fig. 3 displays discharge profiles at different times in order to follow not only the progression of the discharge flooding wave but also the effect of the secondary hydrographs entering at later times through the tributary creeks. It is also worth noting the torrential character of the flow in this simulation, hence the inherent numerical difficulties, as indicated by the Froude number distribution along the valley at an intermediate time during the simulation Fig. 1. This figure also indicates the

supercritical regime at the downstream end.

The second step, was the definition of different scenarios oriented to flood risk mitigation. The first was to model the effects of the construction of an in-line reservoir as storage structure at the upstream inlet making use of the extremely wide natural cross section in that part. We shall call this solution 1 (s1). In a different approach, the second flood mitigation measure introduced in our model was the hypothesis of upstream reforestation. This will be called solution 2 (s2). The assumption of a change in the land use and vegetation over the area forming the basin draining into the upper part of the creek modified the parameters defining the soil infiltration capacity so, for identical rain conditions, led to smaller peak hydrographs. As the third and last risk mitigation strategy, a roughness reduction in the channelized part was proposed by means of bank vegetation clearing and concrete cover. This will be referred to as solution 3 (s3). This option was simulated by means of a modified Manning roughness coefficient in the lower 3 Km, reducing the original n=0.03 to n=0.015. A direct comparison of the results obtained from the three hypothetis is shown on Fig. 2, where the maximum wetted cross section distributions are compared and on Fig. 3, where the maximum discharge distributions are compared.

# 5 Conclusions

A finite volume based numerical technique has been applied as a CFD tool for evaluating different flood risk remediation strategies in a low mountain area. The computational model solves the unsteady shallow water equations in presence of dry bed and irregular topography. It has proved robust, useful and efficient as a predictive tool being able to handle transcritical flow situations keeping the mass error balance close to machine accuracy.

# References

[Burguete (2001)] Burguete J. and García Navarro P., Efficient construction of high-resolution TVD conservative schemes for equations with source terms. Application to shallow water flows, *Int. Journal for Numerical Methods in Fluids, 37, 209-248*, 2001.

[Chanson (1999)] Chanson H., The hydraulics of open channel flow, *Arnold*, 1999.

[Chow et al. (1994)] Chow V.T., Maidment D.R. and Mays L.W., Applied Hydrology, *McGraw Hill*, 1994.

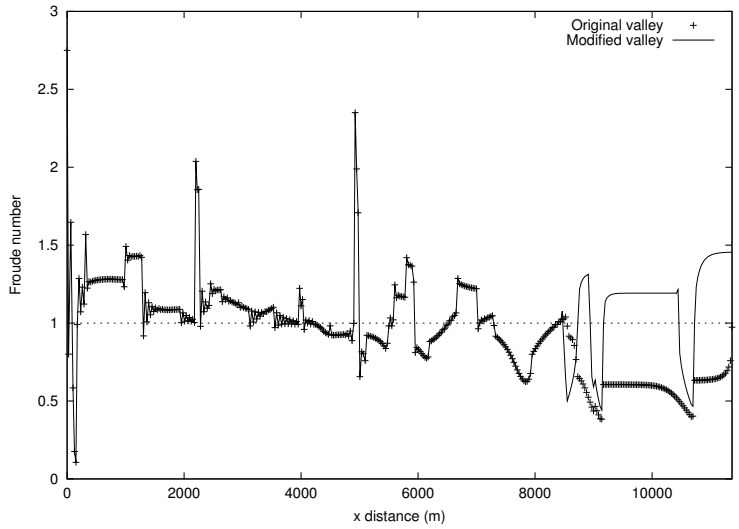


Figure 1: Froude number distribution at time $t = 4 : 00h$ in the basic case.

[Garcia-Navarro et al. (1999)] Garcia-Navarro P, Fras A. and Villanueva I., Dam-break flow simulation: some results for one-dimensional models of real cases, *Journal of Hydrology*, *216*, 227–247, 1999.

[García Navarro and Vázquez Cendón (2000)] García Navarro P., and Vázquez Cendón M. E., On numerical treatment of the source terms in the shallow water equations, *Computers and Fluids*,*126*, 26–40, 2000.

[Katopodes, N. and Schamber (1983)] Katopodes, N. and Schamber, D.R., Applicability of Dam-break Flood Wave Models.*Journal of Hydraulic Engineering*, *109,5*, 1983.

[Leveque (1998)] LeVeque R. J., Balancing source terms and flux gradients in high-resolution Godunov methods: the quasi-steady wave-propagation algorithm,*Journal of Computational Physics*, *146(1)*, 346–365, 1998.

[Roe (1981)] Roe, P. L., Approximate Riemann solvers, parameter vectors, and difference schemes,*Journal of Computational Physics*, *43(2)*, 357–372, 1981.

[Toro (2001)] Toro E., Shock- Capturing Methods for Free- Surface Shallow Flows,*Wiley,*, UK, 2001.

[Vázquez-Cendón (1999)] Vázquez-Cendón M. E., Improved treatment of source terms in upwind schemes for the shallow water equations in channels with irregular geometry, *Journal of Computational Physics*, *148(2)*, 497–526, 1999.

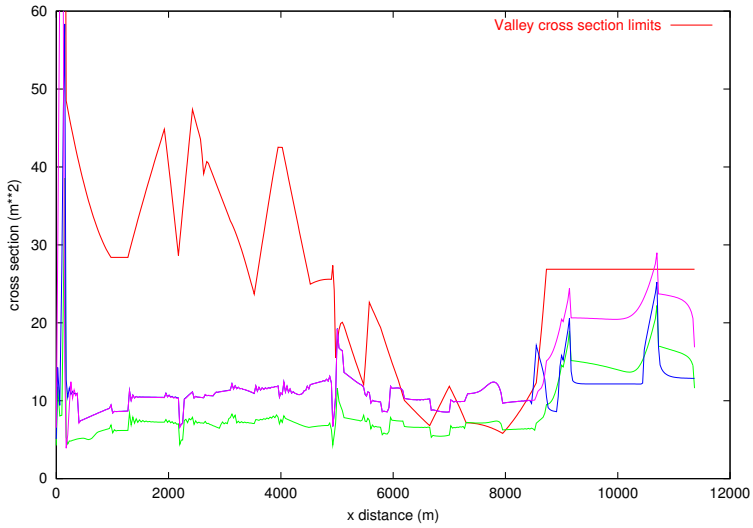


Figure 2: Valley cross section (red line) and water cross section profiles at time $t = 4:00$h for s1, s2 and s3.

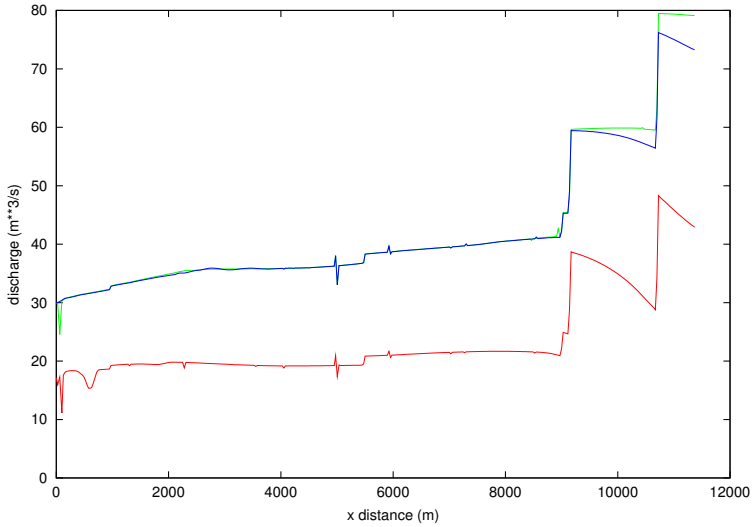


Figure 3: Discharge distribution at time $t = 4:00$h for s1, s2 and s3.